Electronic Supplementary Information for:

Stability, electronic structure, and optical properties of protected gold-doped silver $Ag_{29-x}Au_x$ (x = 0-5) nanoclusters

Rosalba Juarez-Mosqueda,[†] Sami Malola,[†] and Hannu Häkkinen[*†‡]*

[†]Department of Physics and [‡]Department of Chemistry, Nanoscience Center, University of Jyväskylä, FI-40014 Jyväskylä, Finland

TABLE OF CONTENTS

Figure S3. Angular-momentum-resolved PLDOS per atom type and per phenyl ring of the **1D**, **2D**, **4D**, **5D**, **3F**, and **3H** structures.

Figure S4. Evolution of the optical spectra of doped $[Ag_{29-x}Au_x(BDT)_{12}(TPP)_4]^{3-}$ nanoclusters (x=2-4) with respect to the number of Au-TPP bonds.

Table S1. Relative energies and HOMO-LUMO energy gaps (given in parentheses) of $[Ag_{29-x}Au_x(BDT)_{12}(TPP)_4]^{3-}$ nanoclusters with x=2-4. The formula $Ag_{29-x}Au_x@Sn$ indicates the number of Au atoms (x) at each cluster shell (*Sn*) *n* being from 0 to 3. **xE-xH** are the labeling to specify the number of Au dopants and the type of structure. Values in bold correspond to the relative energies and HOMO-LUMO energy gaps calculated with the van der Waals functional. All energies are expressed in eV per cluster.

	[xE]	**[xF]**	**[xG]**	**[xH]**
	$Ag_{29-x}Au@S0$-$Au_{x-1}@S2$	**$Ag_{29-x}Au@S0$-$Au_{x-1}@S3$**	**$Ag_{29-x}Au@S0$-$Au_{x-2}@S1$-Au@*S2***	**$Ag_{29-x}Au@S0$-$Au_{x-2}@S1$-Au@*S3***
x = 2	0.243 (1.810)	0.369 (1.820)	----	----
x = 3	0.449 (1.825) **1.501 (1.699)**	0.777 (1.818) **0.942 (1.693)**	0.236 (1.831) **0.340 (1.740)**	0.386 (1.799) **0.613 (1.733)**
x = 4	0.560 (1.871)	1.125 (1.811)	0.236 (1.799)	0.348 (1.786)

Table S2. Atomic charges (in a.u.) of the $[Ag_{29-x}Au_x(BDT)_{12}(TPP)_4]^{3-}$ nanoclusters with structures of type **1A**, **2A**, **3A-3D**, **4A**, and **5A**. The values are the average of the atomic charges per atom type at each shell. Average atomic charges of the P, C, and H atoms in the TPP molecule are shown as reference.

atoms@shell	**Ag_{29}**	**1A**	**2A**	**3A**	**3B**	**3C**	**3D**	**4A**	**5A**	**TPP**
Ag@S0	-0.0731	----	----	----	0.0165	-0.0572	-0.0561	----	----	----
Au@S0	----	-0.3714	-0.343	-0.3096	----	----	----	-0.2975	-0.2607	----
Ag@S1	0.1257	0.1480	0.1600	0.1738	0.1667	0.1256	0.1256	0.1883	0.1996	----
Au@S1	----	----	-0.1197	-0.1224	-0.1326	----	----	-0.1027	-0.0890	----
Ag@S2	0.3045	0.3069	0.3088	0.3111	0.3131	0.3244	0.3088	0.3112	0.3116	----

Au@S2	----	----	----	----	----	0.0655	-----	----	----	----
Ag@S3	0.3203	0.3300	0.3254	0.3262	0.3253	0.3213	0.3181	0.3287	0.3317	----
Au@S3	----	----	----	----	-----	----	0.0500	----	----	----
S	-0.2890	-0.2841	-0.2827	-0.2811	-0.2790	-0.2646	-0.2753	-0.2808	-0.2731	----
P	1.4928	1.4667	1.5102	1.5020	1.5072	1.4998	1.5945	1.5313	1.4692	1.3824
C	-0.1033	-0.1055	-0.1078	-0.1063	-0.1041	-0.1051	-0.1053	-0.1042	-0.1057	-0.1311
H	0.0601	0.0622	0.0645	0.0631	0.0600	0.0614	0.0629	0.0600	0.0633	0.0651

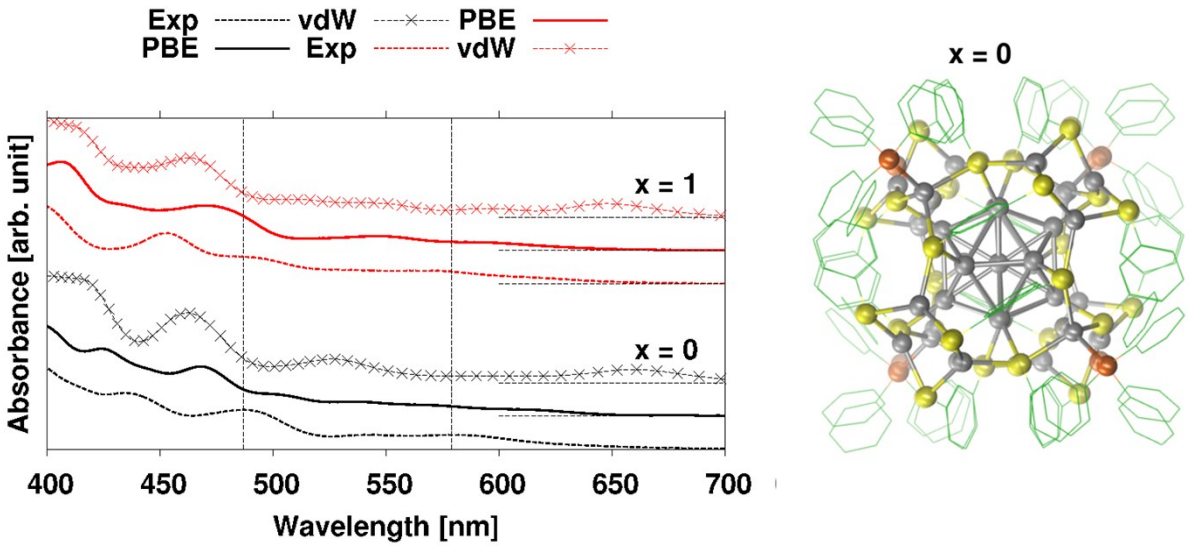

Figure S1. (Left) Comparison between the optical spectra of $[Ag_{29-x}Au_x(BDT)_{12}(TPP)_4]^{3-}$ nanoclusters, with x = 0 (black) and x = 1 (red), calculated using the experimental crystal structure (dashed lines), and the optimized structures with the PBE (solid lines) and the van der Waals functional (x-dashed lines). Vertical-dashed line intersecting at 487 nm and 579 nm indicate the main absorption peaks of the experimental $[Ag_{29}(BDT)_{12}(TPP)_4]^{3-}$ structure. Horizontal-dashed lines show the zero value of the absorbance in each plot. (Right) the overlap of the $[Ag_{29}(BDT)_{12}(TPP)_4]^{3-}$ structures optimized with the PBE and the van der Waals functionals.

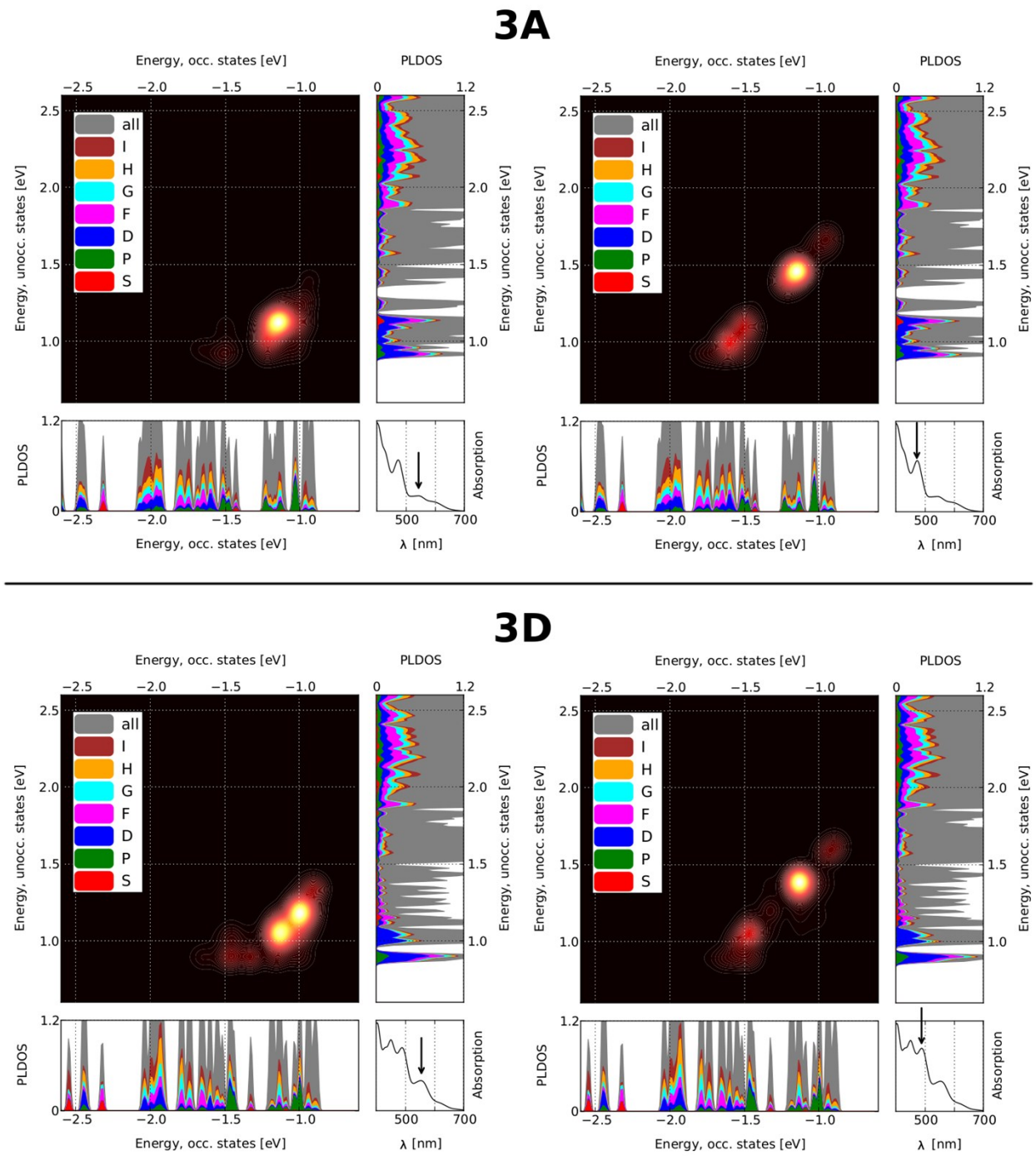

Figure S2. Transition contribution map for the spectral features of the $[Ag_{26}Au_3(BDT)_{12}(TPP)_4]^{3-}$ nanoclusters with structures **3A** and **3D**. The electronic transitions are analyzed at 543 nm and 472 nm (**3A**), and at 555 nm and 488 nm (**3D**). The angular-momentum-resolved (Y_{lm}) PLDOS of the occupied (bottom-left) and unoccupied (top-right)

KS states are shown below and next to the TCM. The arrows in the optical spectra (bottom-right) point to the analyzed absorption peak.

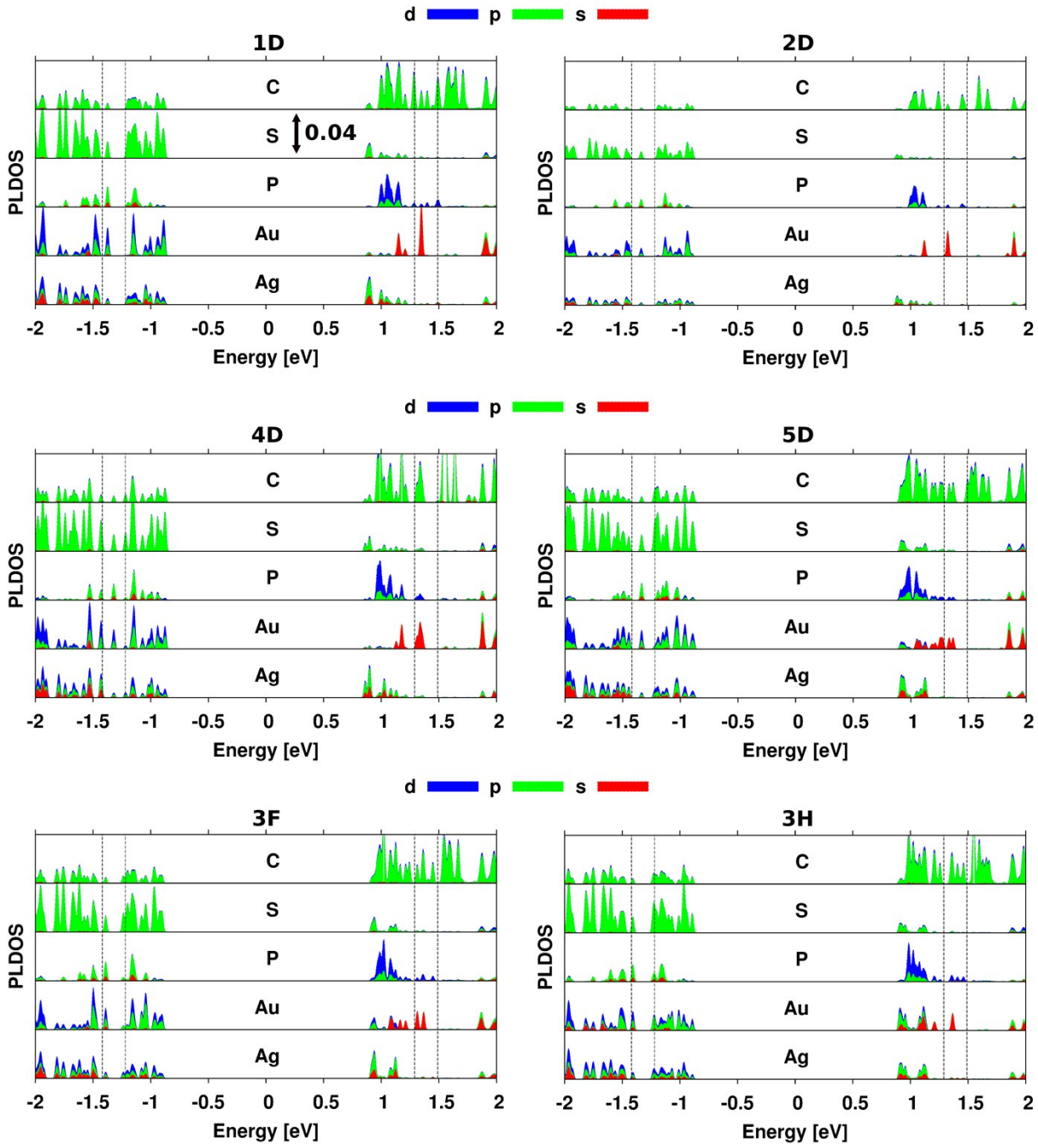

Figure S3. Angular-momentum-resolved (Y_{lm}) PLDOS per atom type (Ag, Au, P, S), and per phenyl ring (in the case of C) of the **1D**, **2D**, **4D**, **5D**, **3F**, and **3H** structures. Blue, green, and red within the plots represent the density

of the atomic s, p and d states. Dashed lines enclosure the occupied and unoccupied states around -1.32 eV and 1.39 eV, respectively. Up-down arrow shows the $Y_{lm} = 0.04$ scale of each plot.

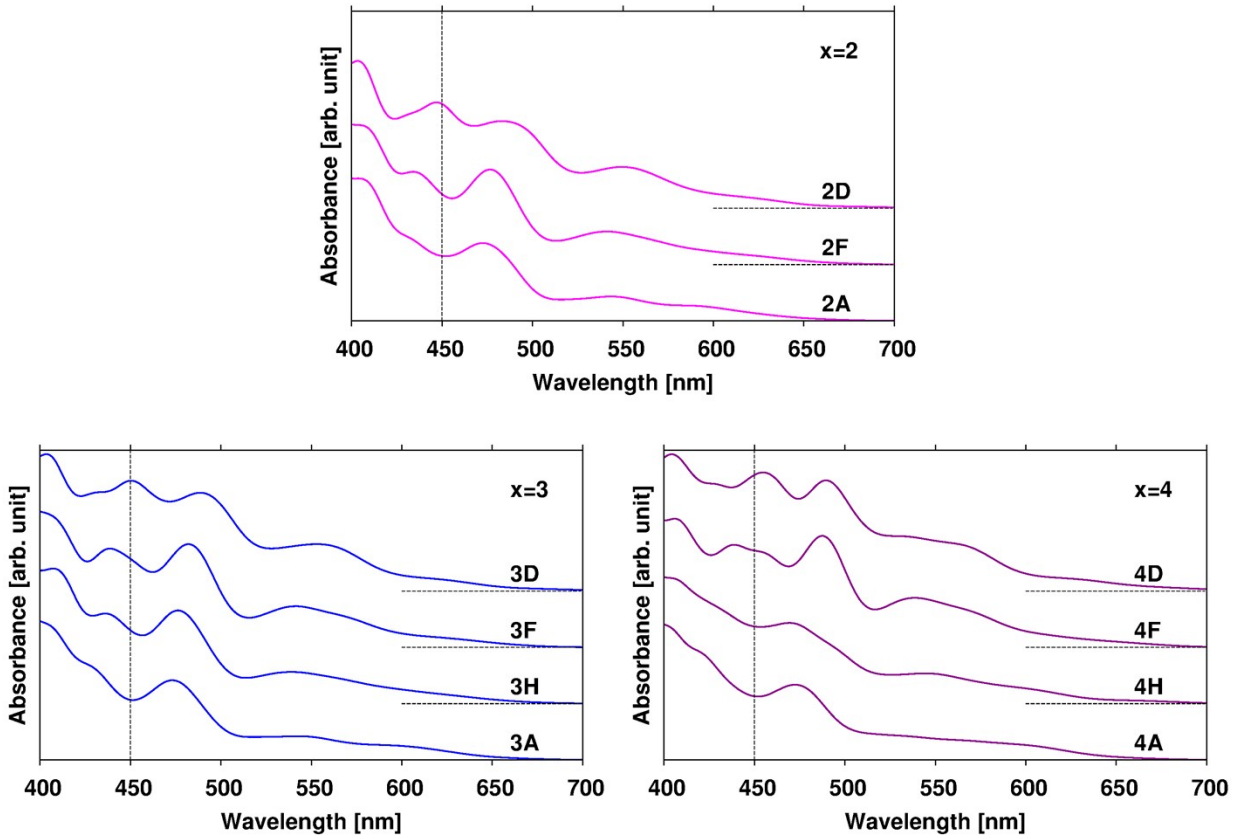

Figure S4. Evolution of the optical spectra of doped $[Ag_{29-x}Au_x(BDT)_{12}(TPP)_4]^{3-}$ nanoclusters (x=2-4) with respect to the number of Au-TPP bonds. The optical spectra corresponds to structures with zero (**2A, 3A,** and **4A**), one (**2F**, **3H**, and **4H**), two (**2D** and **3F**), three (**3D** and **4F**), and four (**4D**) Au-TPP bonds. Vertical-dashed line intersecting at 450 nm is used to indicate the relative shift of the absorption peak related to the Au-TPP bonding in the doped structures.